Strojniški vestnik - Journal of Mechanical Engineering 56(2010)10, 599-608
UDC 004.032.26:681.5
Paper received: 07.12.2009
Paper accepted: 01.10.2010

Improved Micropositioning of 2 DOF Stage by Using the Neural Network Compensation of Plant Nonlinearities

Jure Čas[1,*] - Gregor Škorc[2] - Riko Šafarič[1]
[1] University of Maribor, Faculty of Electrical Engineering and Computer Science, Slovenia
[2] RESISTEC UPR d.o.o. & Co.k.d., Slovenia

This paper describes the system for micropositioning of a 2 DOF mechanism with piezoelectric actuators (PEAs) called a piezo actuated stage (PAS). The PAS is fabricated by a photo structuring process from photosensitive glass and PEAs are built-on to meet the request for its precise movement. The PAS is designed as a general 2 DOF stage. It can be used for different micropositioning or micro-assembling tasks according to the selected end-effector. The other components of the closed-loop control system for micropositioning of PAS are the high voltage drivers, the incremental position sensors and the control processing unit. Due to the nonlinear behaviour of the system for micropositioning, the precise position control of PAS with traditional PI controller is aggravated. Concerning the plant nonlinearities, the feedforward neural networks (NN) are used as a tool for their compensation. After the training procedure with the back-propagation (BPG) algorithm, the trained NN inverse model of plant nonlinearities is used as a feedforward part of the proposed controller. The experiment results have shown that the NN compensation improves the control performance of traditional PI controller.

Keywords: piezo actuated stage, position control, hysteresis, feedforward neural networks

0 INTRODUCTION

Micropositioning is advanced technology, which is used in many research laboratories and companies, especially for the microscopy and advanced electronics manufacturing. The micropositioning systems are also employed in every day devices such as hard discs, camcorders, cars, etc. The usability of these devices depends on their precise movement, usually with submicron resolution. A micropositioning stage generally refers to a system which can automatically move an end-effector in its workspace with submicron resolution. For micropositioning stages it is desirable that they have high resolution, large workspace and compact size. The applications with micropositioning stages have already been reported [1].

There are several different materials and actuation principles for the actuation of micropositioning stages. Due to their nano-metre resolution, high stiffness, big driving force, and fast response PEAs are recognized as fundamental elements for managing extremely small displacements [2]. PEAs are compact and rugged. They exhibit high stability and are practically immune to electromagnetic interference. However, the existence of nonlinear multi-path hysteresis in piezoelectric material aggravates the position control of PEAs in high precision applications. When compared with the maximal displacement of PEAs, the maximum hysteretic error is typically between 15 to 20%. The hysteresis makes it difficult to control the displacement in a case of varying target position because the voltage needed for the desired displacement, is not constant but varies with each actuation and also depends on the history of the motion. Understanding hysteresis behaviour is a fundamental step when designing the position controller for PAS.

Control techniques to reduce the hysteresis effect in PEAs can be divided into four categories, i.e. electric charge control, feedforward (open-loop) position control, feedback (close-loop) position control and combination of feedforward and feedback position control. The electric charge control exploits the fact that the relationship between the position of PEAs and the induced charge has less hysteresis than that between position and applied voltage, as shown in [3] and [4]. However, this approach requires specialized equipment to measure and amplify the induced charge. The feedforward (open-loop) and feedback (closed-

*Corr. Author's Address: University of Maribor, Faculty of Electrical Engineering and Computer Science, Smetanova ulica 17, 2000 Maribor, Slovenia, jure.cas@uni-mb.si

loop) controllers, which are utilized with high-voltage drivers, are mainly studied with the systems with PEAs.

The feedforward controllers are known for their many advantages. The instability problem, which is presented in feedback controllers, is avoided with the feedforward controllers. Furthermore, the accurate and usually expensive position sensors are not needed. Instead of measuring the actual submicron displacement, the feedforward controllers are based on different hysteresis models, which can be approximated, for example, by the polynomial approximation [5], least-mean-square (LMS) algorithm approximation [6] etc. Among the proposed hysteresis models, the *Preisach model* [7] is by far the most well known and widely used. The subclass of the *Preisach model* is *Prandtl-Ishlinskii model* [8], which is less complex. Furthermore, the inverse of *Prandtl-Ishlinskii model* can be computed analytically, thus making it more attractive for real-time applications. However, the feedforward controllers, which are designed for hysteresis compensation, are generally not appropriate for systems with changing load and environment parameters, i.e. changing plant model. Additionally, the creep of PEAs, which can be described as a slow variation of displacement under constant voltage, aggravates the usability of open-loop controllers.

The feedforward controllers are known for their many advantages, but with regard to the described restrictions, they are usually employed for positional control of systems with the PEAs. The PI controller [9] is a proven control technique, which is, owing to its simplicity and reliability, utilized with the majority of the control applications. The parameters of PI controller are usually tuned to match the overshoot and rise-time criteria. According to the hysteresis nonlinearity, the tuning of these parameters is not a trivial problem for the systems with PEAs. Furthermore, the constant parameters of a PI controller cannot assure the optimal performance of the controller over the whole workspace.

In order to make a good use of feedforward control (hysteresis compensation) and feedback control, the authors have also proposed the combinations of both techniques. The inverse hysteresis model (e.g. *Preisach model*) can be employed in parallel with the close-loop PI controller [10]. The inverse hysteresis model can also be modelled with the neural networks as in [11]. As a result of this research, authors propose the cerebellar model articulation neural network controller, which can be used for compensation of nonlinearities of the piezo-actuated plant.

The proposed control approach, which is described here, is conceptually similar to that presented in [11], but with other important differences. Instead of cerebellar model articulation neural networks, the feedforward NN are used for the hysteresis compensation. The NN training by the back-propagation algorithm is similar to that described in [12]. The proposed training is executed before the control process as a sort of controller calibration. The NN model is used in combination with the linear PI controller. It is proven by experiments that NN compensation of plant nonlinearities improves the control performance of linear PI controller.

Section 1 describes the PAS and other components of the closed-loop control system for micropositioning, i.e. the experimental set-up. Section 2 describes the nonlinear characteristic of the controlled plant. Section 3 describes the short theory of the NN and the training configuration. Section 4 describes the control results of PI controller and PI controller combined with NN hysteresis compensation. The control experiments prove the usability of the proposed control scheme. Section 5 gives some final conclusions.

1 SYSTEM FOR MICROPOSITIONING

The PAS consists of a parallel glass mechanism (PGM) and two PEAs. The PGM is similar to a parallelogram. It is designed to transmit the displacement of PEAs on the tip displacement of the PAS, where the end-effector can be mounted. Due to its mechanical construction with dual flexure hinges, the motions are limited with only the actuated DOF, i.e. the axes of PAS are not coupled. The PEA A actuates the *X DOF* and PEA B actuates the *Y DOF* on the workspace (Fig. 1).

The PGM [13] is made of a photosensitive glass with a thickness of 1 mm. The photo structuring process, with partial process steps UV-lithography, thermal treatment, and etching, forms the basis for producing micro-structured glass components. The process is based on

different etching rates of exposed and non-exposed glass.

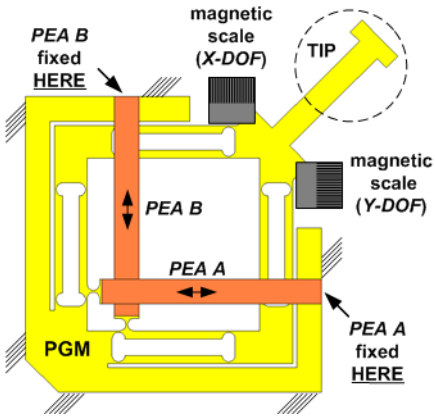

Fig. 1. *Operating principle of PAS (ground plan view)*

Two PEAs with dimensions 27 by 3 mm, with a thickness of 0.2 mm are joined to the PGM. The driving voltages for the PEAs must be inside the maximal driving voltage interval, i.e. from -100 to 100 V. According to the maximum driving voltages, the theoretical displacement of unloaded PEA is ±3.3 μm. However, the maximum displacement of the PEAs is not reached when they are joined to the PGM, because PGM generates a reactive/opposite force similar to the spring force. When the maximum voltage of ±100 V is applied, the maximal theoretical displacement of PEA is ±1.1 μm only. By the transmission rule, the displacement of the PEAs is multiplied by a transmission ratio of PGM. The theoretical tip displacement over one DOF is approximately ±15 μm. Accordingly, the theoretical workspace of PAS is equal to square with 30 μm long sides as described in [12].

The PAS is designed as a general purpose micropositioning device. Its practical usage depends on the type of the end-effector on the tip. The PAS can be mounted on the mechanical stage of a microscope as the specimen holder in order to guarantee an effective microscopy of the specimen. The approximate positioning of PAS with specimen can be provided with the fine adjustment knob of the microscope, while the precise positioning of the specimen can be provided by PAS. The specimen positioning can be referenced by using the graphical user interface running on the desktop computer. The other hypothetical use of PAS can be utilized by using the micro-gripper, which is also made of a photo-sensitive glass. The micro-gripper is actuated with PEAs. The whole system can be used as a tool for handling micro-sized objects. It is described in greater detail in [14].

Precise micropositioning of PAS is a complicated task due to the plant nonlinearities. In order to guarantee the precise micropositioning of PAS, the voltage drivers, incremental position encoders and appropriate control processing unit are developed as components of a close-loop control system. Fig. 2 shows the close-loop control system and the data flow between the components. The host computer is used as a user interface for programming the control processing unit and for the user interaction with the PAS.

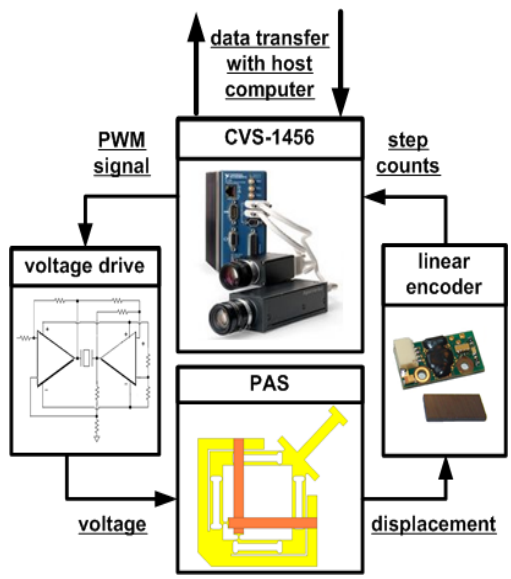

Fig. 2. *The close-loop control system with PAS*

The Compact Vision System (CVS) from the *National Instruments* is used as a control processing unit [15]. Voltage drivers are developed based on the operational amplifiers from the *Apex Microtechnology* [16], and the position measuring is established based on the incremental encoders from *NANOS Instruments GmbH* [17].

Developed voltage drivers have two parts, i.e. signal electronics and power electronics parts. The signal electronics part is designed to filter the reference pulse width modulated (PWM) signal to the corresponding voltage within ±10 V. The

power electronic part is designed to amplify the voltage within ±10 V to driving voltage by differential pairing of operational amplifiers. Two operational amplifiers with part number *PA-78* from *Apex Microtechnology* are configured in a bridge circuit [18]. In this configuration, the operational amplifiers supply an output-voltage swing twice that of a single operational amplifier.

The system for measuring the actual position of PAS with submicron resolution is based on the linear incremental encoders. The linear encoder works on a magnetic principle with a resolution of 0.061 μm. Two magnetic scales are fixed on the PAS perpendicularly, while two belonging encoder sensors are fixed on the base. The vertical distance between the magnetic scales and the encoder sensors is less than 0.1 mm. The magnetic scale moves under the encoder sensor without any mechanical contact. Each pair of sensor and magnetic scale is used to measure one DOF. The photo of PAS with incremental encoders is shown in Fig. 3.

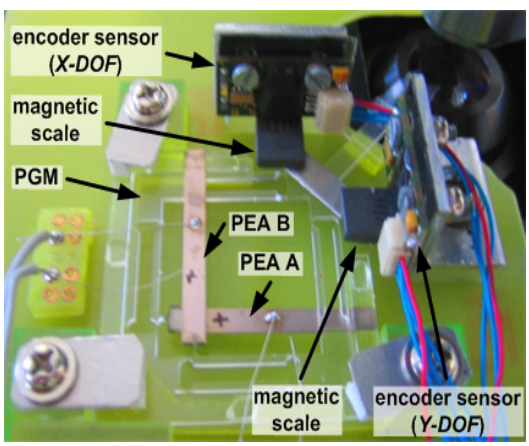

Fig. 3. *PEA with linear incremental encoders*

The CVS is equipped with 15 digital input lines and with 14 digital output lines. Two PWM output signals with frequency 100 kHz are generated for two voltage drivers. On the other hand, two pairs of encoder signals are used to sample the position of PAS. The maximal sampling frequency of input signals equals 100 kHz. According to this, the maximum detected speed of PAS in one direction is 6.1 mms^{-1}.

In order to make the system for micropositioning robust and autonomous, the CVS is configured as a stand-alone processing unit. The communication with the host computer is established through the Ethernet port with the TCP/IP server-client communication protocol.

The user can manipulate with the PAS through the user interface application which runs on the host computer. The actual user interface application is adopted to measure the control performance with the proposed controllers. The user interface can be simply adopted for other micropositioning or micromachining applications like the microscopy image acquiring.

2 DESCRIPTION OF NONLINEAR PLANT

The PWM duty cycle-displacement characteristic of the PAS is mainly affected by the highly nonlinear hysteresis effect of piezoelectric material. The developed close-loop control system was used for measuring the nonlinear positioning behaviour of PAS. Fig. 4 shows 6 successive point-to-point (PTP) movements, i.e. the movement trajectories for *X DOF* with respect to the PWM duty cycle.

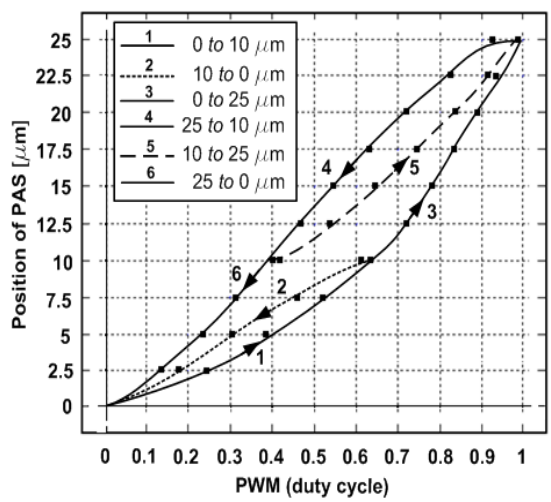

Fig. 4. *Graph of PWM duty cycle vs. displacement (X DOF)*

The above experiment shows that the PAS displacement mainly depends on the PWM duty cycle (driving value) and on the history of motion. In order to describe and evaluate the history of motion, the definition of extreme points, i.e. position turning values, is introduced. The turning values are classified into two categories, i.e. as upper turning values (X_{TU} or

Y_{TU}) and lower turning values (X_{TL} or Y_{TL}). Turning values indirectly describe the level of saturation of PEAs, which depends on the strength of the applied electrical field. Physically it is presented as friction between the moving crystals in the piezo material structure.

The hysteresis effect renders impossible to precisely set the desired position of PAS without using an appropriate position controller. This is also proved with the experiment (Fig. 4), by which it is clearly seen that the actual position of 15 µm, is achieved with different driving values of PWM duty cycle, i.e. 0.79, 0.55 and 0.65.

The simple linear feedforward controller (LFFC) is used in the following experiments as a part of NN training configuration which is described in the section below (Fig. 6). At the beginning of the LFFC design, the size of the PAS workspace is defined with four boundary pairs, i.e. the lower and the upper boundary of workspace for *X DOF* and the lower and the upper boundary of workspace for *Y DOF*. For each of these four boundary pairs, the corresponding driving value (PWM duty cycle) is measured. Accordingly, four boundary pairs are defined as $\mathbf{P^X_{min}}\left(b^X_{min}, dv^X_{min}\right)$, $\mathbf{P^X_{max}}\left(b^X_{max}, dv^X_{max}\right)$, $\mathbf{P^Y_{min}}\left(b^Y_{min}, dv^Y_{min}\right)$ and $\mathbf{P^Y_{max}}\left(b^Y_{max}, dv^Y_{max}\right)$, where b is a boundary and dv is a driving value. The boundary pairs are used as the parameters of LFFC, which is defined as:

$$LFFC^X = dv^X_{\min} + \frac{dv^X_{\max} - dv^X_{\min}}{b^X_{\max} - b^X_{\min}} \cdot X_{ref}\,, \qquad (1)$$

$$LFFC^Y = dv^Y_{\min} + \frac{dv^Y_{\max} - dv^Y_{\min}}{b^Y_{\max} - b^Y_{\min}} \cdot Y_{ref}\,. \qquad (2)$$

Eqs. (1) and (2) define the LFFC output as a straight line through two points (boundary pairs). The LFFC cannot guarantee the appropriate position control for most reference positions on the workspace (Fig. 5).

When the reference position is selected at 10 µm, for example, the LFFC output (driving value) is equal to 0.59. Considering the first '**1**' and the second trajectory '**2**' on the graph, the required driving values to reach this reference position are equal to 0.75 and 0.48, separately. When the LFFC is used, the actual position in the first case equals 6.4 µm (the movement from 2 to 16 µm). In the second case (the movement from 16 to 2 µm), the actual position is equal to 13.8 µm. However, the LFFC is primarily not designed for accurate position control of the PAS, but it is used to train the proposed NN with BPG algorithm. After the training, the NN are used to generate the appropriate output to minimize the position error of PAS. According to this, the PWM duty cycles for driving PAS are defined as follows:

$$PWM^X = LFFC^X + NN^X\,, \qquad (3)$$

$$PWM^Y = LFFC^Y + NN^Y\,, \qquad (4)$$

where PWM^X and PWM^Y are the driving values, $LFFC^X$ and $LFFC^Y$ are the outputs from the LFFC and NN^X and NN^Y are the outputs from the NN for both DOF. Based on NN inputs, the trained NN are capable to generate the appropriate driving values (NN^X and NN^Y). In other words, the NN are capable of estimating and compensating the nonlinear behaviour of PAS.

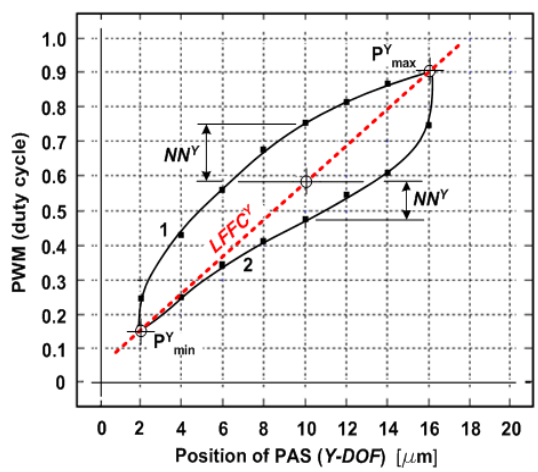

Fig. 5. *The output of LFFC with nonlinear characteristic of PAS*

3 NN TRAINING OF INVERSE MODEL OF PLANT NONLINEARITIES

Any function can be arbitrarily closely approximated by NN that has enough neurons, at least one hidden layer, and an appropriate set of weights [19]. The general modelling capability of NN is a very attractive property for nonlinear approximation problems. Our approach is to

globally linearize the behaviour of the PAS, by training the NN to compensate the hysteresis.

In regards to the observations from the previous section, the plant nonlinearities are mainly dependent on two values, i.e. the reference position value and turning value. Therefore, the input layer of the NN must be defined as:

$$\mathbf{NN_{In}} = \left\{ X^n_{REF}, Y^n_{REF}, X^n_T, Y^n_T \right\}^T, \quad (5)$$

where X^n_{REF} and Y^n_{REF} are normalized reference position values and X^n_T and Y^n_T are normalized turning values of PAS. According to the experiments with the PAS, the accuracy and the speed of the inverse nonlinearities estimation is more effective with 2 NN (Fig. 7). Due to its special mechanical construction with parallel movement, the axes of PAS are not coupled. Therefore, the estimation of inverse nonlinearities with two NN is possible. In order to use two NN, Eq. (5) is modified to Eqs. (6) and (7), which describe the NN input layer:

$$\mathbf{NN_{In}} = \left\{ X^n_{REF}, X^n_T \right\}^T, \quad (6)$$

$$\mathbf{NN_{In}} = \left\{ Y^n_{REF}, Y^n_T \right\}^T. \quad (7)$$

According to [19], two equal NN with three layers of neurons are proposed. The activation function of nodes in the hidden layer (S_H) is a widely used sigmoid function, which is defined as:

$$S_H\left(\mathbf{netJ}\left(j\right)\right) = 1/\left(1+e^{-\mathbf{netJ}(j)}\right), \quad (8)$$

$$\mathbf{netJ}(j) = \sum_{i=1}^{2}\left(\mathbf{w_J}_{ij} \cdot \mathbf{NN_{In}}_{\ i}\right); j = 1 \div n\ , \quad (9)$$

where $\mathbf{w_J}_{ij}$ is the matrix of weights in the hidden layer and n is the number of nodes in the hidden layer. The activation function of the node in the output layer (S_O) is the linear function, which is defined as:

$$S_O\left(\mathbf{netL}\left(l\right)\right) = 0.1 \cdot \mathbf{netL}\left(l\right), \quad (10)$$

$$\mathbf{netL}(l) = \sum_{j=1}^{n}\left(\mathbf{w_L}_{jl} \cdot S_H\left(\mathbf{netJ}\left(j\right)\right)\right), \quad (11)$$

where $\mathbf{w_L}_{jl}$ is the matrix of weights in the output layer and r is the number of nodes in the output layer, and it is equal to 1.

For an estimation of the inverse nonlinearities of the controlled object (PAS), the BPG [20] is used as a training algorithm of NN. The BPG algorithm is summarized as:

$$\Delta\mathbf{w}^p_{L\,jl} = \varepsilon \cdot \dot{S}_O\left(\mathbf{netL}\left(l\right)\right) \cdot e \cdot S_H\left(\mathbf{netJ}\left(j\right)\right), \quad (12)$$

where $\Delta\mathbf{w}^p_{L\,jl}$ is the matrix of weight's variations of the output layer and ε is the learning rate value. The error (e) is a measurement of how far away a particular solution (output of NN) is from a desired solution. Furthermore, the variations of the weights in the hidden layer are defined as:

$$\Delta\mathbf{w}^p_{J\,ij} = \varepsilon \cdot \dot{S}_H\left(\mathbf{netJ}\left(j\right)\right) \cdot \mathbf{NN_{In}}_{\ i} \cdot \cdot \sum_{j=1}^{n}\left(e \cdot \dot{S}_O\left(\mathbf{netL}\left(l\right)\right) \cdot \mathbf{w_L}_{\ jl}\right), \quad (13)$$

where $\Delta\mathbf{w}^p_{J\,ij}$ is the matrix of the weight's variations of the hidden layer. At the end of each iteration step (p) the weight matrixes are updated as:

$$\mathbf{w}^{p+1}_{L\,jl} = \Delta\mathbf{w}^{\,p}_{L\,jl} + \mathbf{w}^{\,p}_{L\,jl}, \quad (14)$$

$$\mathbf{w}^{p+1}_{J\,ij} = \Delta\mathbf{w}^{\,p}_{J\,ij} + \mathbf{w}^{\,p}_{J\,ij}. \quad (15)$$

The updated weight matrixes are used in the following iteration step (p+1).

The BPG is a supervised training algorithm of NN. In the supervised training, the actual output of NN is compared with the target output, which is provided by the external teacher (supervisor). Depending on those two values, the error is defined and back-propagated in order to decrease it in every iteration step of the training process.

However, in our application we use a gradually different procedure of training with BPG algorithm. The error is not defined as the difference between the target output and the actual output of NN, but it is measured on-line, based on the step response of LFFC (Fig. 6).

According to the proposed training configuration, the errors are defined as:

$$e^X = X^n_{REF} - X^n_{ACT} \text{ for } 1^{\text{st}} \text{ NN and} \quad (16)$$

$$e^Y = Y^n_{REF} - Y^n_{ACT} \text{ for } 2^{\text{nd}} \text{ NN.} \quad (17)$$

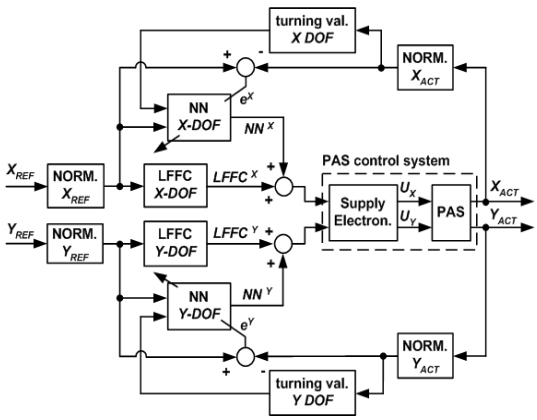

Fig. 6. *The NN training configuration*

The errors are defined as the difference between the reference position value and the actual position value of the PAS for each DOF.

The NN training is executed by using the train data set, which consists of randomly distributed train data pairs defined as $\mathbf{T}^{\mathbf{X}}\left(X^n_{REF}, X^n_{TV}\right)$ and $\mathbf{T}^{\mathbf{Y}}\left(Y^n_{REF}, Y^n_{TV}\right)$. During the training, train data pairs are randomly selected from the train data set and the BPG is repeated on the selected train data pair. After a 100 repetitions of the BPG training algorithm, the new train data pair is selected and the BPG training procedure is repeated.

The learning ability of NN is measured with the sum square error (*SSE*), which is defined by the following equation:

$$SSE^X = \sum_{i=1}^{500}\left(\left(X^n_{REF} - X^n_{ACT}\right)^2\right), \qquad (18)$$

$$SSE^Y = \sum_{i=1}^{500}\left(\left(Y^n_{REF} - Y^n_{ACT}\right)^2\right), \qquad (19)$$

where *i* is the number of measurement. Due to the maximum number of measurements (500), it is evident that the *SSE* is summed-up for every five successive train data pairs from the train data set. Fig. 7 shows three different measurements of *SSE*. The lower two lines show the measurements of SSE^X and SSE^Y separately. The upper line shows the measurement of SSE^{INN} when only one NN with 4 inputs and 2 outputs is used for the estimation of plant nonlinearities. According to *SSE* measurements, we decided to use two NN for hysteresis compensation (each for one DOF).

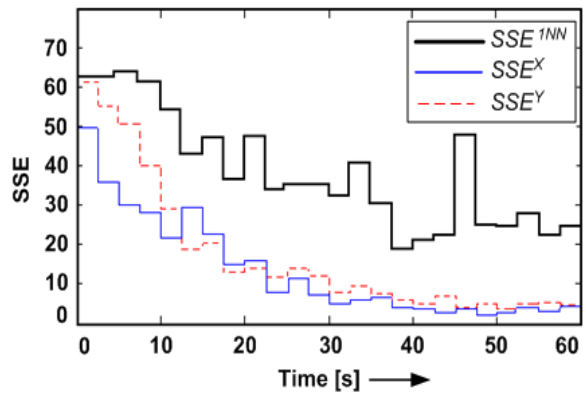

Fig. 7. *Measurement of SSE*

According to the *SSE* measurements, the NN are unable to completely approximate the inverse nonlinearities of PAS. The *SSE* values are more than zero after 60 seconds of the approximation process, and they do not decrease significantly after this time period. However, at *SSE* decreased to some minimal value, we manually stop the learning and save the trained weights of NN into a folder on a disc.

4 FEEDBACK POSITION CONTROL

Since LFFC, combined with the NN compensation, is not able to completely remove the control error of PAS, the LFFC is replaced with a feedback PI controller. A PI and PID controller, respectively, are robust control techniques widely used in the industrial applications. PID controller involves three separate parts, i.e. the proportional part (P) determines the reaction to the current error, the integral part (I) determines the reaction based on the sum of recent errors, and the derivative part (D) determines the reaction based on the rate at which the error has been changing.

In the proposed control application, the derivative gain value is eliminated because it does not have a significant influence on control performance. The optimal proportional gain value (K_P) and the integral time value (Ti) must be determined to assure the optimal control performance of the selected PI controller.

The Ziegler-Nichols closed loop tuning method [9] is a proven heuristic method for online tuning of P, PI and PID controllers. However, by involving the constant parameters (K_P and Ti), the control performance of linear PI

controller cannot be equal (optimal) over the whole workspace of PAS. In order to avoid this restriction, the PI controller is combined with the NN compensation of plant nonlinearities (Fig. 8).

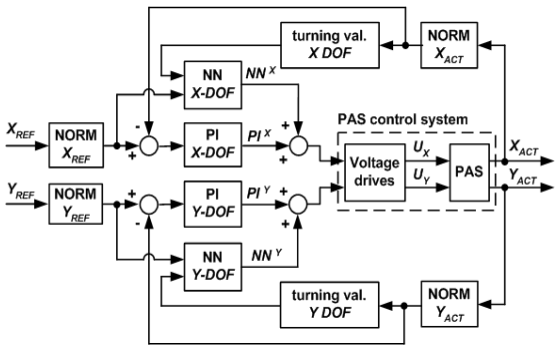

Fig. 8. *Feedback control scheme*

By using the Ziegler-Nichols tuning method, the approximate parameters of the PI controller were first calculated. Furthermore, the parameters of the PI controller and the PI controller with NN compensation were manually tuned on-line by using the step responses with reference positions 5 and 10 µm.

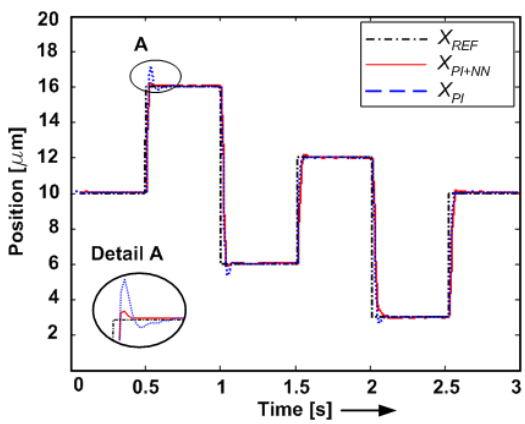

Fig. 9. *PTP response of the controlled system with PI controller and PI controller with NN compensation (X DOF)*

The following experiments show the PTP responses of the controlled system with PI controller and PTP responses of PI controller with NN compensation for arbitrary reference positions on the workspace for *X DOF* (Fig. 9) and for *Y DOF* (Fig. 10). The aim of experiments is to provide the PTP responses without an overshoot over the whole workspace, as this is significant for micropositioning with any micropositioning device.

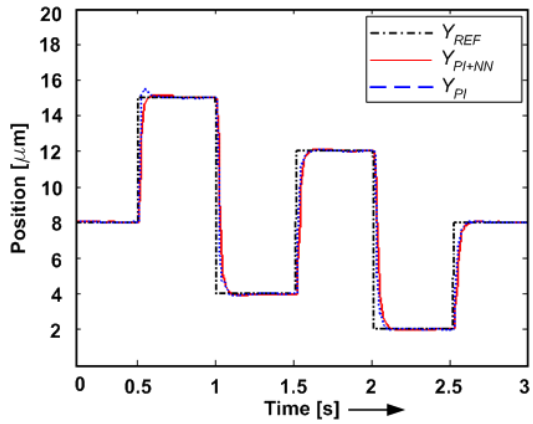

Fig. 10. *PTP response of the controlled system with PI controller and PI controller with NN compensation (Y DOF)*

The PTP responses with PI controller at 1.5 and at 2.5 seconds are almost ideal, but the PTP responses at 0.5 seconds and at 1.0 seconds exhibit large overshoots (Fig. 9). When PI controller is used, the overshoot is also obtained in the Fig. 10.

When the PI controller with NN compensation is used, the PTP response of the controlled system is equal (without overshoot) for all reference positions on the workspace. Therefore, the NN compensation of plant nonlinearities improves the step response of the controlled system with PI controller.

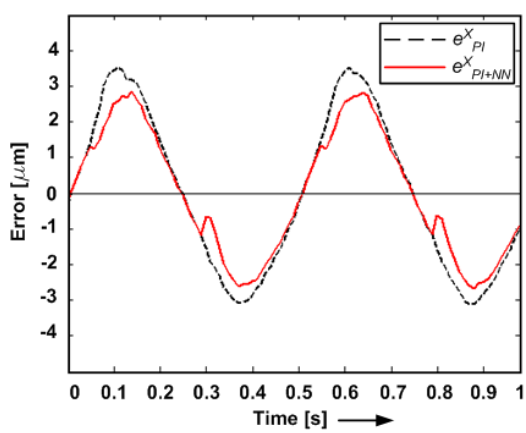

Fig. 11. *TT with PI controller and with PI controller with NN compensation (X DOF)*

Figs. 11 and 12 show the trajectory tracking (TT) errors of the system with the PI controller and the PI controller with NN compensation. The reference position is described as a circular movement with a radius of 7.5 µm and circular frequency 2 Hz.

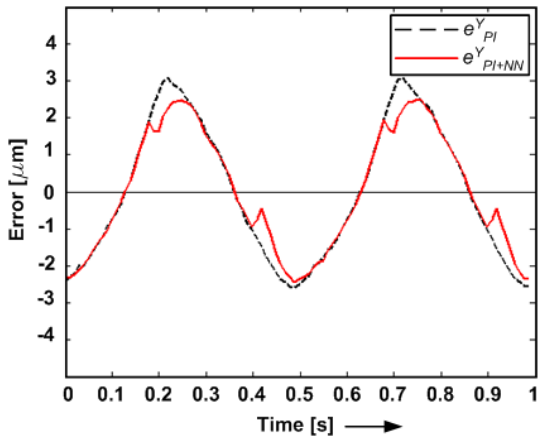

Fig. 12. *TT with PI controller and with PI controller with NN compensation (Y DOF)*

The experiments show that maximum error decreases by 20 % when NN compensation is included into the control scheme.

The presented results show that the proposed NN compensation of hysteresis improves the control performance of the traditional PI controller. The experiments have shown that the control performance of linear PI controller is more stable over the whole workspace of PAS.

5 CONCLUSION

The first part of the presented research focuses on the development of the system for close-loop micropositioning. The presented observations may provide readers with some useful information when designing their own micropositioning systems. Furthermore, the development of an appropriate position controller of PAS is described. The experiments in section 2 clearly show that PAS displacement is a nonlinear function of driving values (PWM duty cycle) and position turning values. The proposed method focuses on the development of the inverse model of hysteresis, which is used as a feedforward part of the proposed controller. However, the inverse hysteresis model with the mathematical functions is complicated to model thus, the NN are used. The experiments in section 4 show the control results of the linear PI and PI controller with the NN hysteresis compensation. It is evident that the additional NN compensation of plant nonlinearities improves the control performance of linear PI controller.

6 REFERENCES

[1] Yang, R., Jouaneh, Z., Schweizer R. (1996). Design and characterization of a low-profile micropositioning stage. *Precision Engineering*, vol. 18, p. 20-29.

[2] Yao, O., Dong, J., Ferreira, P. (2007). Design, analysis, fabrication and testing of a parallel-kinematic micropositioning XY stage. *International Journal of Machine Tools and Manufacture*, vol. 47, no. 6, p. 946-961.

[3] Comstock, R.H. (1981). *Charge control of piezoelectric actuators to reduce hysteresis effects*, U.S. Patent num.: 4,263,527.

[4] Ronkanen, P., Kallio, P., Koivo, H. (2002). Current Control of Piezoelectric Actuators with Power Loss Compensation. *IEEE/RSJ International Conference on Intelligent Robots and System*, Lousanne.

[5] Chonan, S., Jiang, Z., Yamamoto, T. (1996). Nonlinear hysteresis compensation of piezoelectric ceramic actuators. *Journal of Intelligent Material Systems and Structures*, vol. 7, no. 2, p. 150-156.

[6] Ru, C-H., Sun, L., Kong, M. (2005). Adaptive inverse control for piezoelectric actuator based on hysteresis model. *Proc. of 4th Int. Conf. on Machine Learning and Cybernetics*, Guangzhou.

[7] Weibel, F., Michellod, Y., Mullhaupt, P., Gillet, D. (2008). Real-time compensation of hysteresis in a piezoelectric-stack actuator tracking a stochastic reference. *American Control Conference*, Washington.

[8] Krejci, P., Kuhnen, K. (2001). Inverse control of systems with hysteresis and creep. *IEE Proceedings - Control Theory Applications*, vol. 148, no. 3, p. 185-192.

[9] Zigler, J.G., Nichols, N.B. (1942). Optimum settings for automatic controllers. *American Society of Mechanical Engineer*, p. 759-768.

[10] Ge, P., Jouaneh, M. (1996). Tracking control of a piezoceramic actuator. *IEEE Transactions on Control Systems Technology*, vol. 4, no. 3, p. 209-216.

[11] Ku, S.-S., Pinsopon, U., Cetinkunt, S., Nakajima, S. (2000). Design, fabrication, and real-time neural network control of a three-degrees-of-freedom nanopositioner. *IEEE/ASME Transactions on Mechatronics*, vol. 5, no. 3, p. 273-280.

[12] Čas, J., Škorc, G., Šafarič, R. Neural network position control of XY piezo actuator stage by visual feedback. *Neural Computing and Applications*, vol. 19, no. 7, p. 1043-1055.

[13] Keoschkerjan, R., Qiao, F., Wurmus, H. (2000). Piezoelectric XY-Micropositioner made of photosensitive glass to form one micro-handling unit. *Proceedings of 7th International Conference on New Actuators*, Bremen.

[14] Keoschkerjan, R., Wurmus, H. (2002). A novel microgripper with parallel movement of gripping arms. *Proceedings of 8th International Conference on New Actuators*, Bremen.

[15] NI CVS-1450 Series User Manual. From *http://www.graftek.com/pdf/Brochures/NationalInstruments/cvsmanual.pdf*

[16] Power Operational Amplifiers (*PA-78*). From *http://www.cirrus.com/en/pubs/proDatasheet/PA78U_B.pdf*

[17] Linear Encoders. From *http://www.nanos-instruments.de/nanosweb/media/pdf/Encoder_engl_v4.pdf*

[18] PA78 Design Ideas. From *http://www.cirrus.com/en/pubs/appNote/AN_PA78_Design_Ideas.pdf*

[19] Hornik, K., Stinchombe, M., White H. (1989). Multilayer feedforward networks are universal approximator. *Neural Networks*, vol. 2, p. 359-366.

[20] Hecht-Nielsen, R. (1989). Theory of backpropagation neural network. *Proc. of Int. Joint Conf. on Neural Networks*, Washinghton DC.